PCCP

Accepted Manuscript

ROYAL SOCIETY OF CHEMISTRY

www.rsc.org/pccp

PCCP

COMMUNICATION

Metal Adatoms Generated by Co-play of Melamine Assembly and Subsequent CO Adsorption

Received 00th January 20xx,
Accepted 00th January 20xx

DOI: 10.1039/x0xx00000x

www.rsc.org/

Li Wang,[a] Qi-wei Chen,[b] Hong Shi,[a] Hui-hui Liu,[a] Xinguo Ren, [c,d,*] Bing Wang, [e] Kai Wu,[b,f,*] and Xiang Shao[a,*]

Molecular self-assembly films are expected to tailor the surface process by the periodic nanostructures and add-on functional groups. In this work, a molecular network of melamine with featured pores of subnanometer size is prepared on Au(111) surface, and is found to be able to trap the gold adatoms and concomitant single vacancies generated under the impingement of CO molecules at room temperature. DFT calculations suggest that the strong CO-Au-adatom interaction as well as the high adhesion of Au adatom inside the melamine pore could well be the driving force behind such process. This study not only sheds light onto the interactions between gasses and the metal surface that is covered by molecular self-assembly films, but also provides a novel route to manipulate the monoatomic surface species which is of catalytic interest.

Metal adatoms play important roles in heterogeneous catalysis. Both monoatomic metal species on oxide supports, and the intrinsic adatoms on bare metal surfaces provide essential active sites for molecular bindings and subsequent reactions.[1-3] It is generally accepted that, at least on bare metal surfaces, there are a vast number of adatoms in balance with surface defects including step edges, kinks, dislocations, etc.[4] For coinage metals such as Au, Ag and Cu, there exists a close relationship between their surface activities and the mobile adatoms. Both Ag and Cu adatoms are heavily involved in catalytic oxidation reactions.[5-7] Au, inert as a bulk material, exhibits considerable catalytic activity when its surface is nanostructured and populated with low-coordinated sites particularly the adatoms.[8, 9]

The concentration of adatoms is normally affected by the surface environments such as surface orientation, temperature, exposed pressure, and so on.[10, 11] It is recently reported that the exposure to CO can induce self-healing of a sputtered Au(111) surface, which is exactly mediated by the surface Au adatoms.[12] However, this process obviously counters against the desired reactivity due to the elimination of the low-coordinated sites and recovering of the close-packed surface. Oppositely, creation of adatom species or redistribution of the metal loadings is expected to enhance the reactivity, which thus attracts more and more attentions.[13] For instance, modifying the metal species with surface adhesive ligands can effectively increase the binding strength of the metal adatoms to the substrate and hence prevent their aggregation. A number of single atomic catalysts have been successfully prepared in this scenario.[1,14] In addition, preparation of nanoporous structures at the oxide surfaces has also been proved to be an effective strategy to trap single metal adatoms on the oxides.[15-17] Self-assembled molecular grids incorporated on surfaces, on the other hand, provide a more flexible option since the well-defined atomic traps can be readily constructed by depositing designed molecules.[18-20]

By subtly tuning the intermolecular interactions from van de Waals to hydrogen bonding, and from metal-ligand coordination to covalent bonding, various molecular assembly structures have been successfully constructed.[21,22] The networks with periodic cavities represent one type of the most attractive assembly structures. The tuneable pores can either hold adaptable anchoring sites for either guest molecules or particles, or provide synergistic microenvironments which facilitates novel chemical reactions.[23] Melamine (1,3,5-triazine-2,4,6-triamine) is one of such typical building blocks for hydrogen-bonding based nanostructures. Its co-assemblies with other molecules are often explored to control the deposited guest molecules such as C_{60} and thiols.[24,25] Particularly, intrinsic gold adatoms on bare Au(111) surface

---

[a] Department of Chemical Physics, University of Science and Technology of China, Hefei 230026, China E-mail: shaox@ustc.edu.cn
[b] BNLMS, College of Chemistry and Molecular Engineering, Peking University, Beijing 100871, China E-mail: kaiwu@pku.edu.cn
[c] Key Laboratory of Quantum Information, University of Science and Technology of China, Hefei 230026, China E-mail: renxg@ustc.edu.cn
[d] Synergistic Innovation Center of Quantum Information and Quantum Physics, University of Science and Technology of China, Hefei 230026, China
[e] HFNL, University of Science and Technology of China, Hefei 230026, China
[f] Singapore Peking University Research Centre (SPURc), 1 CREATE Way, #15-01, CREATE Tower, 138602, Singapore

† Electronic Supplementary Information (ESI) available: Additional STM images. Fig. S1. STM images obtained at different biases showing the distinctive morphologies of the second-layer melamine and ABS. Fig. S2. Series of STM images showing bias-dependent morphology of the Au adatoms. Fig. S3. Calculated model showing CO absorbing in melamine pores with flat-lying configuration. See DOI: 10.1039/x0xx00000x

can be effectively trapped inside the hexagonal melamine pores during the film growth.[26, 27] Here in this paper, we report another novel strategy to manipulate the metal adatoms. By dosing CO to the melamine self-assembly monolayer on Au(111), we can create the gold adatoms and concomitant atomic vacancies in a controlled manner.

The experiments were performed on a low-temperature scanning tunnelling microscope (LT-STM, Createc Co.) which is housed in a UHV chamber with base pressure lower than 1 × 10^{-10} mbar. Atomically flat Au(111) surface was prepared by repeated cycles of Ar+ sputtering and annealing. The melamine molecules (Aldrich, 99%) were thoroughly degassed at 100℃ inside a Knudsen-cell type evaporator for 10 hours in vacuum before deposition. To prepare a pure honeycomb-structured melamine film the substrate was kept at around 500 K during evaporation. CO (Air Product, 99.999%) was introduced to the sample surface by background feeding through a variable leak valve. The partial pressure of CO was controlled at 1.0×10^{-5} Pa ~ 1.0×10^{-4} Pa and the samples were kept at room temperature. All STM measurements were conducted at liquid nitrogen temperature. The STM images were collected with the electrochemically etched tungsten tips in constant current mode.

Melamine is reported to form two kinds of typical assembly structures on Au(111) surface, i.e. close-packed (C-Mel) and honeycomb (H-Mel) ones, depending on the employed coverage and other controlling conditions.[27] In our experiments, deposition of melamine at elevated substrate temperature (around 500 K) resulted in a pure H-Mel film with minimum intrinsic gold adatoms. Fig. 1a shows such a film imaged by high resolution STM where each melamine molecule appears as a triangular protrusion. The repeating unit can be defined as an antiparallel molecular pair connected by two N-H…N hydrogen bonds (see the model in the inset of Fig. 1a, the hydrogen bonds are marked by the red dashed lines). These molecular pairs arrange into a diamond pattern and form an extended two-dimensional honeycomb structure. The close-packed directions of the honeycomb orientate along the <21$\overline{3}$> directions of the Au(111) surface, forming an angle of about 15° against the ridges of the $(22\times\sqrt{3})$ reconstructed herringbone structures, i.e. the <11$\overline{2}$> directions of the Au(111) surface.

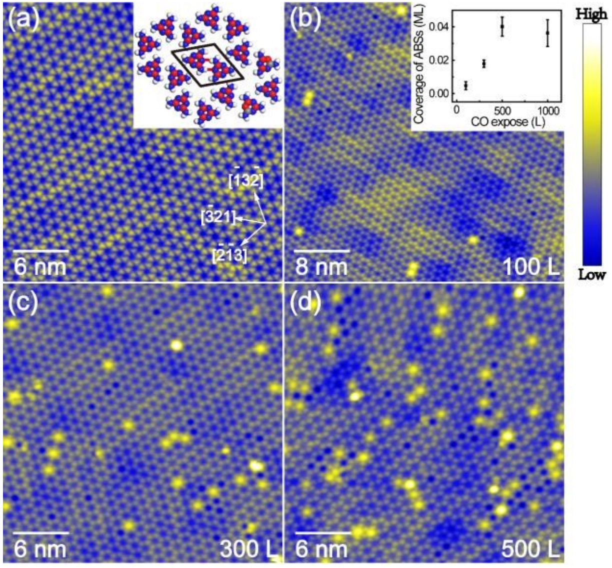

Figure 1. STM images of (a) bare H-Mel film on Au(111) and (b-d) after exposure to different amount of CO at RT. The inset in (a) shows molecular model of H-Mel structure (red, blue and white balls for C, N, and H atoms, respectively). Short red lines mark the N-H…N hydrogen bonds. The diagram in (b) shows the coverage of the ABSs as a function of CO exposure. Tunnelling conditions: (a) I = 100 pA, U = 0.3 V; (b) I = 270 pA, U = 2 V.

All measured structural parameters are in line with previous reports.[27] Nevertheless a surprising finding is that many added bright spots (ABSs) appear after exposing the H-Mel film to a CO atmosphere at room temperature. Figs. 1b-1d show the results after dosing different amount of CO, wherein the numbers of the emerged ABSs rise almost linearly with the CO exposure at the early stage, but quickly saturate at further exposures. The saturated concentration of the ABSs under our experimental condition reached around 0.04 ML (monolayer) after exposing to 1000 L (Langmuir, 1 L = 10^{-6} Torr • sec) of CO. As can be seen in the images, the ABSs are precisely positioned at the centres of the melamine pores and display uniformly atomic size, namely 0.5 nm for the diameter and 0.07 nm for the height under usual imaging conditions. Therefore, one monolayer of ABS means every melamine pore is filled with one ABS. In previous studies of melamine assemblies on Au, similar bright spots were observed when depositing melamine with very low speed and low coverage. Those bright spots were attributed to intrinsic surface gold adatoms that are captured by melamine molecules during the film growth.[26,27]

What are these added species here? The first plausible answer may be the adsorbed CO molecules in consideration of the positive correlation between their concentration and the CO exposure. However, this conjecture is not consistent with the weak binding strength of CO with either the gold surface or the melamine molecules. Melamine has never been reported to absorb CO even under ambient conditions. Moreover, numerous experimental and theoretical studies have demonstrated extremely weak adhesion of CO to the Au(111) surface.[28] Substantial CO adsorption at room temperature can be completely excluded on perfect Au(111) terraces but was observed on the stepped or sputtered gold samples which are defective surfaces featured with many low-coordinated gold atoms.[29] In contrast, the melamine-covered Au(111) surface in our experiments still shows perfect terraces with rare defects, as shown in Fig. 1a. And the ABSs distribute evenly on the large domains of the H-Mel film, showing no connection to any intrinsic surface defect at all. Therefore it's not plausible to assign them as the trapped CO inside the pores. With similar arguments, but also through a series of control experiments, other potential gaseous adsorbates which were possibly introduced during CO dosing can all be safely excluded.[30]

The second possible explanation of the ABSs may be the trapped melamine molecules. It has been frequently reported that various molecules could be trapped to the pores of the H-Mel films.[26,27,31] Previously on Ag(111) the second-layer melamine was proposed to account for the added species observed on the H-Mel film at raised coverage.[32] Under our experimental conditions, we can also prepare the second-layer melamine by evaporating excessive amount of molecules onto the full-coverage H-Mel film. However, as shown in Fig. S1, these second-layer melamine molecules present a bias-independent height of around 170 pm, which is much higher than the above-mentioned ABSs, ruling out the possibility that they are the second-layer melamine molecules.

Excluding the above two explanations, a closer examination of our bias-dependent STM image data reveals a third and most appealing explanation of the nature of these ABSs. Fig. 2 shows the morphological evolution of the ABSs as a function of the imaging bias while the set-point current is roughly unchanged. The line profiles across the ABSs at the centres of the melamine hexagonal pores are displayed in Fig. 2f. A clear suppression of the brightness was evidenced by the decrease of the height from roughly 70 pm to 20 pm as the bias was reduced from 2.0 V to about 50 mV. More importantly, the morphologies of the ABSs at low biases perfectly match those of the Au adatoms that are trapped inside the melamine pores on the same surface as reported in previous studies.[26,27] In a control experiment, we prepared a sample with a small number of intrinsic gold adatoms by following the reported recipe of depositing melamine film at room temperature with a very low speed.[26] As shown in Fig. S2, these intrinsic gold adatoms show exactly the same bias-dependent brightness as the CO-induced ABSs, suggesting the same nature. We also note that in the previous works of Nilius et al. similar bias-dependent morphological contrast of gold adatoms have been demonstrated on both NiAl(110) and FeO(111) ultrathin film.[33,34] Based on all these evidences, we therefore propose that the ABSs are actually the generated Au adatoms induced upon CO exposure.

CO-induced surface reconstruction is frequently observed and reported on transition metals. It may also take place on the coinage metals, but usually needs high partial pressure up to 1 torr.[35] A recent sum-frequency-generation study reports that there are a remarkable number of short-lived CO-Au species on the sputtered Au(111) surface even under very small CO partial pressure. These species disappear immediately upon removal of CO from the UHV chamber.[12] Studies carried out at more open gold surfaces such as Au(110) and (210) also demonstrated significant interactions of CO with the under-coordinated gold atoms.[36] On the close-packed Au(111) surface, however, no such interaction has been reported or even expected at CO exposure up to ambient pressure. Having these knowledge in mind, the proposed generation of gold adatoms upon exposing CO to the melamine-covered Au(111) surface seems still a striking result. A plausible explanation may have to be seated on the co-play effect of both CO and the existing melamine monolayer. The corresponding mechanism will be discussed in the following.

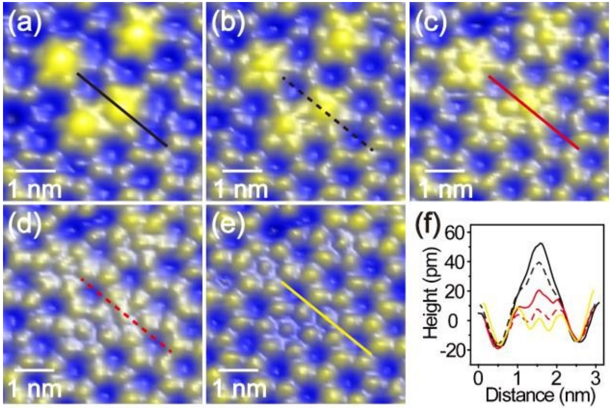

Figure 2. (a) - (e) Bias-dependent STM image sequence of the ABSs. (f) The profiles of the same ABS imaged at different biases: black (a, 2.0 V), dashed black (b, 1.5 V), red (c, 1.0 V), dashed red (d, 0.5 V) and orange (e, 50 mV). Set-point current: (a) 50 pA, (b-c) 60 pA, (d) 80 pA and (e) 120 pA.

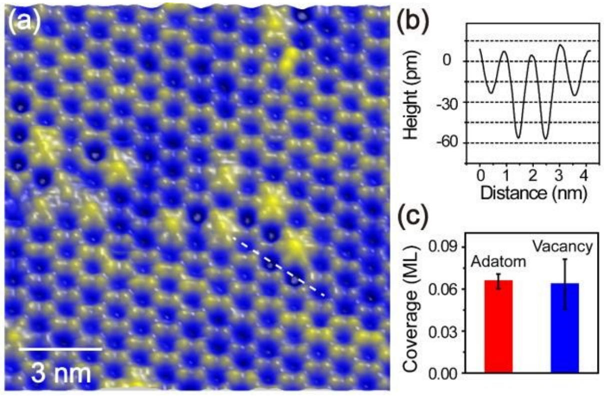

Figure 3. (a) STM image showing the CO-induced gold adatoms and the simultaneously formed vacancies. Tunnelling condition: I = 50 pA, U = 1.6 V. (b) The profile along the white dashed line in (a), which runs across two common pores and two vacancies. (c) Statistical histogram of CO-induced adatoms (red) and the yielded vacancies (blue).

To unravel the formation mechanism of the gold adatoms the first question to answer is where they come from. On bare substrates, the adatoms are usually generated from the surface defects such as steps, kinks, dislocations, etc. When strong ligands are present for chemical bonding, the terrace atoms can also be lifted up and reorganized together with the molecules. In our case, the gold steps were undisturbed even after the surface was exposed to thousands of Langmuirs of CO, in disagreement with the normal step-kink mechanism for adatom generation. On the other hand, melamine is not a strong ligand to gold but interacts rather weakly to the latter.[26,37] Nevertheless, a close look at the film after CO exposure reveals that a significant number of dark species inside the melamine pores are formed simultaneously with the adatoms, as shown in Fig. 3a, which are about 40 pm deeper than the normal melamine pores. More interestingly, these dark species are always closely positioned at and keep 1:1 ratio with respect to the CO-induced gold adatoms, as shown in Figs. 3a and 3b. The concomitant yield of these dark species and their depressive morphologies strongly suggest that they be single atomic gold vacancies inside the melamine pores where the original gold atoms have been transported to neighbouring pores and hence become adatoms. This is truly beyond expectation since the adsorbate-induced surface reconstructions were usually found in strong-interaction systems, such as thiol-Au, amino-Cu etc. However, here in our case both melamine and CO molecules are obviously weakly interacting with the Au surface and cannot create such adatom-vacancy pairs independently. Such a prominent effect can only be attributed to the cooperative work of both melamine and CO molecules.

To understand better the generation mechanism of gold adatoms and unravel the roles played by CO and the H-Mel monolayer, we have performed DFT calculations with the Perdew-Burke-Ernzerhof (PBE)[38] generalized gradient approximation as implemented in the all-electron FHI-aims code package.[39,40] The van der Waals interactions are accounted for in terms of the Tkatchenko-Scheffler (TS) scheme,[41] modified to account for the screening effect of metal surfaces (the so-called vdW^{surf} method).[42,43] The Au(111) surface is modelled by 3-layer Au slabs with (8×8) surface unit cell. Six melamine molecules are deposited onto each surface unit cell, and they form a hexagon structure, as shown in Fig. 4. A single CO molecule is placed inside the pore of the melamine hexagon. Geometry relaxation is carried out using the PBE+vdW method with the lower two Au layers fixed, and is considered converged when all the force components are below 0.05 eV/Å. The calculated adsorption and formation energies of various species are summarized in Table 1. The adsorption energy is defined as the energy difference before and after a CO molecule is adsorbed, whereas the formation energy is defined as the energy difference before and after the creation of an adatom-vacancy pair (AD-Vac) in the system.

Table 1. Calculated adsorption/formation energies by PBE and PBE+vdW methods.

ΔE(eV)	CO(s)/Au(111)[a]	CO(s)/Mel/ Au(111)[a]	CO(s)/AD-Vac/ Mel/Au(111)[a]	AD-Vac/ Mel/Au(111)[b]
PBE	-0.21	-0.18	-0.96	1.25
PBE+vdW	—	-0.60	-1.18	1.61

a, adsorption energy; b. formation energy

As shown in Fig. 4, after the geometry optimization, the melamine molecules lie flat on the Au surface and the CO molecule also adopts a flat-lying configuration at the centre of the molecular hexagon (see Fig. S3 in SI). This is drastically different from the well-known vertical configuration when CO is adsorbed on bare Au(111). Also the adsorption energy of CO was found significantly increased to -0.6 eV (versus -0.2 eV on bare Au).[44] The enhanced adhesion indicates that CO interacts much longer with the melamine-covered surface than with the bare gold surface.

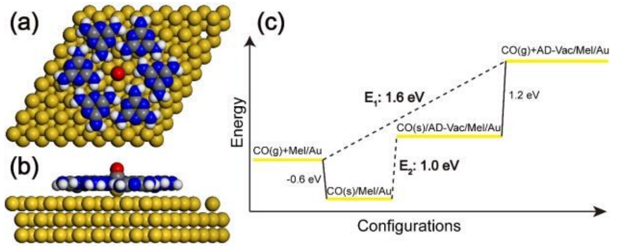

Figure 4. Top view (a) and side view (b) of the calculated configuration of CO adsorbing on a trapped Au adatom in the melamine pore. In the model Au, N, H, O and C atoms are represented by golden, blue, white, red and grey balls respectively. (c) Energetic diagram of various structures with and without CO adsorbed.

The formation energy of an AD-Vac on such a melamine covered surface with (ΔE_2) and without (ΔE_1) CO in presence is calculated respectively as following:

$$\Delta E_1 = E(CO(g)+AD\text{-}Vac/Mel/Au)-E(CO(g)+Mel/Au)$$

$$\Delta E_2 = E(CO(s)/AD\text{-}Vac/Mel/Au)-E(CO(s)/Mel/Au)$$

Here CO(g) means no interaction between CO and the surface, whereas CO(s) means its adsorption on either the bare film or the gold adatom. Notice during the simulation the Au adatom is placed inside while the concomitant vacancy is positioned somewhere outside of the melamine hexagon. The calculated ΔE_1 is around 1.6 eV, which is obviously well beyond the thermal energy at room temperature. However, when CO is present, the formation energy of an AD-Vac is drastically reduced to 1.0 eV (ΔE_2), as depicted in the diagram in Fig. 4b. The large energy gain can be attributed to the strong chemical bond formed between CO and the Au adatom, which restores the vertical configuration of CO on the bare Au(111) surface but with significantly reduced C-Au-adatom distance, as shown in Fig. 4a. Therefore, when CO molecules are continuously exposed to the melamine-covered Au surface at a sufficiently high pressure, the formation probability of CO-Au-adatom species can dramatically increase by a few orders of magnitude. If one considers further the entropy contribution which is bigger for the surface with defects (adatom plus vacancy) than that without, the probability will be even larger.

In our experiments we notice all the CO molecules finally desorb due to the pumping-off, whereas the gold adatoms are left at the centres of melamine pores even above room temperature. This phenomenon cannot be well explained based on our current calculations. We assume there may be a diffusing transition state between (CO(s)/Mel/Au) and (CO(s)/AD-Vac/Mel/Au) which has sufficiently higher energy than the final state, i.e. (CO(g)+AD-Vac/Mel/Au). Therefore when CO is becoming unavailable in the gas phase, some of the Au-CO species release CO first instead of diffusing across this transition state to heal a vacancy nearby. In this way, the AD-Vac configuration can be retained even after CO is removed. In such process, the melamine network serves as a periodic potential well inhibiting the effective recombination of the Au adatoms with the vacancies, even though it does not have strong interactions with both species.

Conclusions

In summary, we have demonstrated the capability in controlling the generation of surface adatoms by exposing the honeycomb-structured assembly films of melamine on Au(111) to CO. Detailed STM experiments recognized the gold adatoms are produced directly from the gold terrace, concomitantly with the formation of single vacancies which are trapped by the melamine hexagonal pores. The DFT calculations suggest that the strong CO-Au-adatom interaction triggers the generation of the adatom-vacancy configuration under the CO atmosphere, but the melamine assembly network plays the important role in preventing the produced species from recombination after CO is pumped off. Reasonably, other similar porous molecular assemblies may be expected to exert the same effect. Therefore, the findings in this work not only demonstrate the importance of the assembled molecular films in tailoring surface processes, but also provide a new strategy to prepare single atomic metal species. The produced metal adatoms and monoatomic vacancies may register potentially interesting surface reactivity, which awaits further explorations in the near future.

Acknowledgements

We are grateful for the financial support of NSFC (91227117, 21333001, 21133001, 21261130090) and MOST (2011CB808702). X. S. thanks the financial support of the Thousand Talent Program for Young Outstanding Scientists of the Chinese government.

References

1 X.-F. Yang, A. Wang, B. Qiao, J. Li, J. Liu and T. Zhang, *Acc. Chem. Res.* 2013, **46**, 1740-1748.
2 A. A. Herzing, C. J. Kiely, A. F. Carley, P. Landon and G. J. Hutchings, *Science* 2008, **321**, 1331-1335.
3 S. F. J. Hackett, R. M. Brydson, M. H. Gass, I. Harvey, A. D. Newman, K. Wilson and A. F. Lee, *Angew. Chem. Int. Ed.* 2007, **46**, 8593-8596.
4 M. Giesen, *Prog. Surf. Sci.* 2001, **68**, 1-153.
5 K. Kern, H. Niehus, A. Schatz, P. Zeppenfeld, J. Goerge and G. Comsa, *Phys. Rev. Lett.* 1991, **67**, 855.
6 C. I. Carlisle, T. Fujimoto, W. S. Sim, and D. A. King, *Surf. Sci.* 2000, **470**, 15-31.
7 O. Nakagoe, K. Watanabe, N. Takagi, and Y. Matsumoto, *Phys. Rev. Lett.* 2003, **90**, 226105.
8 R. A. Ojifinni, N. S. Froemming, J. Gong, M. Pan, T. S. Kim, J. M. White, G. Henkelman and C. B. J. Mullins, *J. Am. Chem. Soc.* 2008, **130**, 6801-6812.
9 M. Pan, J. Gong, G. Dong and C. B. Mullins, *Acc. Chem. Res.* 2014, **47**, 750-760.
10 P. M. Agrawal, B. M. Rice and D. L. Thompson, *Surf. Sci.* 2002, **515**, 21-35.
11 Y. N. Devyatko, S. V. Rogozhkin and A. V. Fadeev, *Phys. Rev. B* 2001, **63**, 193401.
12 W.-L. Yim, T. Nowitzki, M. Necke, H. Schnars, P. Nickut, J. Biner, M. M. Biener, V. Zielasek, K. Al-Shamery, T. Klüner, M. Bäumer, *J. Phys. Chem. C* 2006, **111**, 445-451.
13 B. Yang, Y. Pan, X. Lin, N. Nilius, H.–J. Freund, C. Hulot, A. Graud, S. Blechert, S. Tosoni and J. Sauer, *J. Am. Chem. Soc.* 2012, **134**, 11161-11167.
14 H. Zhang, T. Watanabe, M. Okumura, M. Haruta and N. Toshima, *Nat. Mater.* 2012, **11**, 49-52.
15 N. Nilius, V. Brázdová, M.-V. Ganduglia-Pirovano, V. Simic-Milosevic, J. Sauer, H. –F. Freund, *New J. Phys.* 2009, **11**, 093007
16 S. Ulrich, N. Nilius, H.-J. Freund, U. Martinez, L. Giordano, G. Pacchioni, *ChemPhysChem* 2008, **9**, 1367–1370
17 Z. Novotny, G. Argentero, Z. Wang, M. Schmid, U. Diebold, G. S. Parkinson, *Phys. Rev. Lett.* 2012, **108**, 216103
18 F. Rosei, M. Schunack, P. Jiang, A. Gourdon, E. Lægsgaard, I. Stensgaard, C. Joachim and F. Besenbacher, *Science* 2002, **296**, 328-331.
19 G. Pawin, K.L. Wong, D. Kim, D. Sun, L. Bartels, S. Hong, T. S. Rahman, C. Carp and M. A. Marsella, *Angew. Chem. Int. Ed.* 2008, **47**, 8442-8445.
20 L. Dong, Q. Sun, C. Zhang, Z. Li, K. Sheng, H. Kong, Q. Tan, Y. Pan, A. Hu and W. Xu, *Chem. Commun.* 2013, **49**, 1735-1737.
21 A. Ciesielski, C.-A. Palma, M. Bonini and P. Samorì, *Adv. Mater.* 2010, **22**, 3506-3520.
22 J. V. Barth, *Annu. Rev. Phys. Chem.* 2007, **58**, 375-407.
23 D. Bonifazi, S. Mohnani, A. Llanes-Pallas, *Chem. Eur. J.* 2009, **15**, 7004-7025.
24 J. A. Theobald, N. S. Oxtoby, M. A. Phillips, N. R. Champness and P. H. Beton, *Nature* 2003, **424**, 1029-1031.
25 R. Madueno, M. T. Räisänen, C. Silien and M. Buck, *Nature* 2008, **454**, 618-621.
26 M. Mura, F. Silly, V. Burlakov, M. R. Castell, G. A. D. Briggs and L. N. Kantorovich, *Phys. Rev. Lett.* 2012, **108**, 176103.
27 F. Silly, A. Q. Shaw, M. R. Castell, G. A. D. Briggs, M. Mura, N. Martsinovich and L. Kantorovich, *J. Phys. Chem. C* 2008, **112**, 11476-11480.
28 F. Mehmood, A. Kara, T. S. Rahman and C. R. Henry, *Phys. Rev. B* 2009, **79**, 075422.
29 J. Hrbek, F. M. Hoffmann, J. B. Park, P. Liu, D. Stacchiola, Y. S. Hoo, S. Ma, A. Nambu, J. A. Rodriguez and M. G. White, *J. Am. Chem. Soc.* 2008, **130**, 17272-17273.
30 The other gasses induced by CO dosing, either exchanged from the wall of or the permanent residuals in the UHV chamber, including H_2, O_2, H_2O, CO_2 and Ar, were all monitored with QMS (Quadruple Mass Spectrometer) and confirmed at a reasonable low level during CO exposure. Control experiments by dosing individually these gasses up to 10 L on to the melamine film were not observed to induce formation of any added species.
31 H.-M. Zhang, Z.-K. Pei, Z.-X. Xie, L.-S. Long, B.-W. Mao, X. Xu and L. S. Zheng, *J. Phys. Chem. C* 2009, **113**, 13940-13946.
32 C. H. Schmitz, J. Ikonomov and M. Sokolowski, *Surf. Sci.* 2011, **605**, 1-6.
33 T. M. Wallis, N. Nilius, W. Ho, *J. Chem. Phys.* 2003, **119**, 2296
34 E. D. L. Rienks,1 N. Nilius, H. –J. Freund, L. Giordano, G. Pacchioni, J. Goniakowski, *Phys. Rev. B* 2009, **79**, 075427
35 L. Piccolo, D. Loffreda, F. J. Cadete Santos Aires, C. Deranlot, Y. Jugnet, P. Sautet and J. C. Bertolini, *Surf. Sci.* 2004, **566**, 995-1000.
36 S. A. C. Carabineiro and B. E. Nieuwenhuys, *Gold Bull*. 2009, **42**, 288-301.
37 M. Mura, N. Martsinovich and L. Kantorovich, *Nanotechnology* 2008, **19**, 465704.
38 J. P. Perdew, K. Burke and M. Ernzerhof, *Phys. Rev. Lett.* 1996, **77**, 3865.
39 V. Blum, R. Gehrke, F. Hanke, P. Havu, V. Havu, X. Ren, K. Reuter and M. Scheffler, *Comput. Phys. Commun.* 2009, **180**, 2175–2196.
40 V. Havu, V. Blum, P. Havu and M. Scheffler, *J. Comput. Phys.* 2009, **228**, 8367-8379.
41 A. Tkatchenko and M. Scheffler, *Phys. Rev. Lett.* 2009, **102**, 073005.
42 V. G. Ruiz, W. Liu, E. Zojer, M. Scheffler and A. Tkatchenko, *Phys. Rev. Lett.* 2012, **108**, 146103.
43 W. Liu, A. Tkatchenko and M. Scheffler, *Acc. Chem. Res.* 2014, **47**, 3369-3377.
44 The evaluation of the adsorption energy of CO on the Au(111) surface is not entirely straightforward. For CO on bare Au(111), it is known that the PBE-GGA functional already slightly overestimates the adsorption energy, and in this case, the vdW correction shouldn't be added. In contrast, when the melamine framework is present, one must add the vdW correction to get the correct geometry and adsorption energy.